PAPER

Check for updates

Unlocking the secrets of high-water barrier stereocomplex polylactide blend extrusion films†

James F. Macnamara, Jr., [ID] [a] Maria Rubino,[a] Matthew Daum,[a] Ajay Kathuria[b] and Rafael Auras [ID] *[a]

Consumers, companies, and governments are becoming more interested in compostable materials as the amount of waste generated from single-use petrochemical-based and non-biodegradable plastics has grown exponentially since 1960. A drawback to compostable flexible option films is the lack of equivalent moisture barrier performance to maintain a comparable shelf life of food products compared with traditional petrochemical-based versions. Stereocomplex PLA (SC-PLA), a combination of the stereoisomers L-PLA (PLLA) and D-PLA (PDLA), offers a potential solution to this problem. This study presents a viable and novel method to cast extrude SC-PLA films without using a masterbatch. For comparison, several blend compositions were produced, including 85/15, 70/30, 50/50, and 30/70 PLLA/PDLA and homo-complex PLLA and PDLA films. The samples were then annealed at 160 °C for 5, 15, and 30 min to understand the effect on the crystallinity (X_c), moisture vapor permeability coefficient (MVPC), and functional and mechanical performance. As expected, the X_c increased for all the samples upon annealing. We observed increased crystallization kinetics in the blended samples, which crystallized in 5 minutes, which can be ascribed to the nucleation effect, while the PLLA and PDLA started crystallizing between 15 and 30 minutes. PDLA acted as a nucleating agent at levels as low as 15% to induce crystallization in ≤5 minutes in the blended samples. We observed a correlation between the crystallization trend of various compositions and MVPC, with the blended annealed films having a significantly better moisture barrier than all the non-annealed films. The increased X_c reduces the strength properties due to higher brittleness associated with the higher X_c. Further optimization is needed to produce fully viable films for commercial applications; however, this work shows pathways to unlock the creation of PLA films with high barriers to water.

1. Introduction

The global flexible packaging industry is expected to grow from approximately $129 billion (USD) in 2020 to roughly $178 billion (USD) by 2027. The growth is attributed to the increased demand in the food, beverage, cosmetic, personal care, and pharmaceutical industries.[1] By 2030, the demand is expected to reach an estimated $272 billion (USD).[2] Along with the growth of plastic usage comes the issue of disposal. According to the U.S. EPA, in 2018, 35.7 million tons of plastic waste were generated only in the U.S., representing 12.2% of the total municipal solid waste (MSW). Of the 35.7 million tons, only 8% were recycled, 16% were incinerated, and 76% were sent to landfills.[3] This lack of recycling has concerned consumers, businesses, and governments and led to an interest in developing industrial compostable polymers that can potentially replace non-biodegradable and fossil-based plastics since they can be disposed of with organic waste when contaminated.[4]

Poly (lactic acid) (PLA) is considered one of the leading candidates to replace fossil-fuel-based polymers since it has the most significant commercial production capacity, with increasing market growth.[5,6] It is used in several industrial applications, including biodegradable thermoplastics and food and agricultural packaging.[7–9] However, there are a few issues with its widespread usage and potentially increased commercialization, including low heat distortion temperature,[10] brittleness,[11] poor thermal and hydrolytic stability,[12] and moderate barrier properties.[13,14]

One potential solution to overcome some of the issues is to combine the two enantiomeric forms of PLA, namely L-PLA (PLLA) and D-PLA (PDLA), to produce stereocomplex PLA (SC-PLA).[15] For a well-blended PLLA and PDLA mixture, multi-

[a]School of Packaging, Michigan State University, East Lansing, MI 48824-1223, USA. E-mail: aurasraf@msu.edu
[b]Industrial Technology and Packaging, California Polytechnic State University, San Luis Obispo, CA, 93407-2311, USA
†Electronic supplementary information (ESI) available. See DOI: https://doi.org/10.1039/d3gc04805e

center hydrogen bonding leads to a potential alternative arrangement of helical chains between L-lactyl and D-lactyl portions with opposing chiral confirmation for PLA stereocomplex formation.[16,17] The stereocomplex formed from the PLLA/PDLA enantiomers allows for improved intermolecular interactions *via* dipole–dipole interaction and hydrogen bonding. A more tightly packed chain conformation results side-by-side within the stereocomplex crystal structure, allowing for improved thermal stability and mechanical properties.[18,19] SC-PLA has a melting temperature (T_m) of approximately 225 °C, while homocrystallite PLA (HC-PLA) melts around 180 °C, exhibiting a 50 °C variance between them.[18] Tensile strength, Young's modulus, and elongation at break of SC-PLA are all reported to improve over HC-PLA.[20] Annealed films, after extrusion, increase crystallinity. So, annealing is a common technique in processing polymers to alter their physical and chemical properties.[21] Producing SC-PLA within the PLA matrix and increasing their crystallinity through annealing can improve barrier properties.[22] The moisture vapor transmission rate (MVTR) of solvent-cast SC-PLA films is 14–23% better than that of HC-PLA, opening new markets in industrial applications such as packaging.[23] The higher the crystallinity of SC-PLA, the better the water barrier properties may be if the rigid amorphous fraction (RAF) – the phase between the crystalline fraction (CF) and the mobile amorphous fraction (MAF) – is fully controlled.[22]

This work aimed to determine the optimal conditions for producing SC-PLA by cast film extrusion and explore potential mechanical and barrier properties enhancements. Others have reported on injection molding and twin-screw extrusion of SC-PLA. Luo *et al.* described the melt processing of PLLA/PDLA to form SC-PLA *via* an injection molding process.[24] Alhaj and Narayan reported a scalable process of SC-PLA by twin-screw extrusion formation of pellets for injection.[25] However, cast extrusion films of SC-PLA have yet to be reported and produced. This work focuses on producing SC-PLA films on a single screw extruder without first making a masterbatch. Blends of 85/15, 70/30, 50/50, and 30/70 PLLA/PDLA, along with PLLA and PDLA, were produced for comparison. Maximizing the amount of PLLA is logical, given its widespread presence in the market, as it is expected to offer advantages in supply chain efficiency and cost.[26] PDLA is currently mainly used for the nucleation of PLLA and for producing SC-PLA but is still in much lower demand in the market.[27] The role of SC-PLA content on the properties of these blends, such as thermal, mechanical, and moisture barrier measurements, was measured and reported.

2. Experimental

2.1 Materials

PLLA (Luminy® L175, ≥99%(L-isomer)), PLLA (Luminy® L130, ≥99%(L-isomer)), PDLA (Luminy® D070, ≥99%(D-isomer)), and PDLA (Luminy® D120, ≥99%(D-isomer)) were supplied by TotalEnergies Corbion (Gorinchem, Netherlands). All homopo-

lymers were crystalline white pellets in appearance, with a reported weight average molecular weight (M_w) of 175 kDa for L175, 130 kDa for L130, 70 kDa for D070, and 120 kDa for D120.[28–31] The resins were used as received. Tetrahydrofuran (THF), HPLC grade and stabilized with butylated hydroxytoluene, was procured from Pharmco (Brookfield, CT).

2.2 Film processing

The PLLA and PDLA resins were dried in a vacuum oven (VWR International, USA) overnight (minimum 12 h) at 60 °C and 24 in-Hg before processing to prevent hydrolytic degradation during processing.[28,29]

Dried PLLA and PDLA resins were processed separately to produce respective cast films. Then, the two isomers in a weight ratio of 85/15, 70/30, 50/50, and 30/70 PLLA/PDLA were weighed and thoroughly mixed in a plastic bag before being introduced into the extruder. Each mix was extruded with a microextruder (Randcastle Extrusion Systems, Cedar Grove, NJ, USA) and made into a cast film as a monolayer film. The extruder has a 1.5875 cm diameter screw, 34 cm³ volume, and a 24/1 L/D ratio. The processing temperature and the extrusion conditions are provided in Table S1 of the ESI† available online.

The machine was allowed to stabilize at a chill roll speed of 10 RPM, and the first film sample was collected. The nip roller speed was increased to 15 RPM and then 20 RPM to obtain samples with the desired film thickness.

2.3 Thermal annealing

Each film sample of approximately 25.4 × 16.5 cm was annealed in a QL438-C hydraulic press (PHI, USA) at 160 °C. Samples were placed between 25.4 × 25.4 cm plates lined with non-stick aluminum foil. The annealing was conducted below the T_m of the HC-PLA, and 160 °C was determined to be the optimal temperature for maximum crystallization without destroying the film's integrity. All the samples were annealed for 5, 15, and 30 min; after annealing in the press, the samples were allowed to cool at ambient temperatures. The annealed samples were stored in a freezer at −20 °C until further analysis.

2.4 Size exclusion chromatography (SEC)

The M_w and the number average molecular number (M_n) of the PLLA and PDLA resins were measured using an SEC system from Waters (Milford, MA, USA) equipped with an isocratic pump, an autosampler, a refractive index detector, and a series of Styragel® columns (Styragel® HR-4, HR-3, HR-2), with a controlled temperature of 35 °C and flow rate of 1 mL min⁻¹. Approximately 20 mg of each resin was dispersed in 10 mL of THF and stored overnight to dissolve. Each sample was filtered, transferred to a 2 mL glass vial, and capped. The M_w, M_n, and the polydispersity index, Đ, were analyzed using the Waters Breeze2 software. Six replicates of each resin were measured.

2.5 Melt flow rate (MFR)

The MFR of each resin was measured using a Ray Ran (New Castle, DE, USA) Melt Flow Indexer MK II Digital Model 2A. MFR was evaluated at 190 °C with a 2.16 kg weight as per pro-

cedure A of the ASTM D1238-20 test standard.[32] At least 8 specimens, each of PLLA and PDLA, were evaluated to obtain a low dispersion on the results.

2.6 Thermogravimetric analysis (TGA)

PLLA and PDLA resin samples were characterized using a Q50 thermogravimetric analyzer (TA Instruments, USA) from 100 to 600 °C at 10 °C min^{-1}, under 50 mL min^{-1} nitrogen gas flow. Three samples (5–10 mg) of each resin were evaluated.

2.7 Differential scanning calorimetry (DSC)

Thermal analysis was conducted using a Q100 differential scanning calorimeter (TA Instruments) with a refrigerated cooling system under a 70 mL min^{-1} nitrogen flow. Resin and film samples, each weighing between 5 and 10 mg, were packed and sealed in a standard aluminum pan and lid. The samples were equilibrated to 20 °C, ramped to 0 °C at 10 °C min^{-1}, ramped to 260 °C at 10 °C min^{-1}, held isothermal for 1 min, ramped to 0 °C at 10 °C min^{-1}, and then to 260 °C at 10 °C min^{-1} for a total of two cycles. The heat of fusion (ΔH) of 100% HC-PLA used for the X_c calculation was 139 J g^{-1}.[18] The ΔH of 100% SC-PLA used for the analysis was 142 J g^{-1}.[18] Three replicates of each resin and film were tested.

2.8 Wide angle X-ray diffraction (WAXD)

The wide-angle X-ray diffraction was analyzed on an AXS D8 Advance X-ray diffractometer (Bruker Co., USA) equipped with a global mirror filter Cu Kα radiation source at 40 kV 100 mA. The diffraction pattern was recorded between a 2θ range from 10° and 40° at a rate of 0.24° min^{-1} and an increment of 0.01°. The instrument worked in combination with Diffrac. Measurement Center version 7.5.0 software (Bruker Co.) to collect the data. One replicate each of PLLA, PDLA, and produced blend compositions, with each annealing time was studied.

2.9 Thickness

Caliper measurements of each film (n = 3) were recorded with a TMI digital micrometer (model 49-70-01-0001; USA).

2.10 Barrier properties

Moisture vapor transmission rate (MVTR) was evaluated for PLLA, PDLA, and the produced blended films on a Permatran-W® 3/34 instrument (MOCON, USA) at 38 °C and 90% RH according to ASTM F1249-20.[33] Six or more replicates were evaluated for each film.

2.11 Tensile strength

Tensile testing was conducted on a Universal Testing System Model #5565 (Instron, USA) and measured according to ASTM D882-18.[34] The samples were evaluated in the machine direction (MD) and cross direction (CD). The initial strain rate was 0.1 mm mm^{-1} min^{-1}. The grip separation was 12.7 cm for the MD samples and 7.62 cm for the CD samples. The annealed samples were not wide enough in the CD to achieve a 12.7 cm grip separation, as recommended by the standard. All non-annealed samples and the 85/15 and 70/30 PLLA/PDLA

samples annealed at 5 and 15 minutes were also tested for comparison. All samples were conditioned at 23 °C and 50% RH for over 40 h before testing. The bluehill version 4.25 software (Instron) is integrated with the Universal Testing System to record and calculate the data. Eight replicates of each variable were evaluated.

2.12 Data analysis

Universal Analysis 2000 software version 4.5A (TA Instruments) was used for analyzing and compiling the DSC and TGA data. DIFFRAC.EVA version 5.1.0.5 (Bruker Co.) was used to evaluate the data generated from the Diffrac.Measurement Center software for the WAXD. Fityk 1.3.1 was used to deconvolute the XRD data for analysis.

MATLAB® (Mathworks®, USA) and Microsoft Excel (Microsoft®, USA) were used to compile the data and create the graphs. SAS® (Cary, NC, USA) was used for the statistical analysis of the data. An analysis of variance (ANOVA) calculation was completed on the tensile strength and permeability measurements.

3. Results and discussion

Making a blended PLA film *via* cast extrusion was initially challenging. At first, only one version of each high M_w PLLA and PDLA were obtained, PLLA (L175) and PDLA (D070), and several trials were conducted to establish the best method to produce SC-PLA films. Due to the markedly different MFRs of PLLA (L175) and PDLA (D070), we tried to produce master-batches in a twin extruder and use the resulting masterbatches to produce SC-PLA. However, due to SC-PLA formation during masterbatch production, we could not cast the films in a single extruder from the masterbatches since the films crystallized in the die. Multiple temperature settings were attempted without success.

Another attempt was to vigorously mix PLLA (L175) and PDLA (D070) in a plastic bag and then cast them in a single extruder. The T_m measured was 176.5 ± 1.3 °C and 177.4 ± 0.5 °C for PLLA and PDLA, respectively, and reported as 175 °C for both resins according to the manufacturer.[30,31] However, due to the different MFRs of PLLA (L175) and PDLA (D070), 3.5 ± 0.3 and 10.0 ± 0.9 g per 10 min (190 °C per 2.16 kg), respectively, a good mixing was not achieved, and the films could not be cast. We tried to extrude it at a lower temperature closer to the T_m of the two resins and then at a higher temperature closer to the T_m of SC-PLA. Still, the MFR was a major issue, regardless of the extrusion temperature. Additional attempts were made, but they were futile.

We then obtained two alternative resins, PLLA (L130) and PDLA (D120), which had similar measured MFRs of 12.1 ± 1.5 and 12.2 ± 1.8 g per 10 min (190 °C per 2.16 kg), respectively, potentially facilitating the extrusion mixing. The data sheet reported the MFR as 10 g per 10 min for both resins (190 °C per 2.16 kg).[28,29] The T_m measured was 176.2 ± 0.5 °C and 179.4 ± 1.2 °C for PLLA and PDLA, respectively, and reported

as 175 °C for both resins according to the manufacturer.[28,29] Table S2 in the ESI† summarizes the MFR data of the four resins. Table S3 and Fig. S1† provide a full characterization of all four resins.

The PLLA (L130) and PDLA (D120) resins with comparable MFR at a similar T_m were crucial for obtaining a homogeneous mixture and optimizing the temperature profile for SC-PLA to be formed during the extrusion process while extruding and casting it into a film in one process. Several trials were needed to optimize the temperature profile: at too low of a temperature, only HC-PLA was achieved, while at high temperatures, the mixture flowed too rapidly and did not form a film.

3.1 Cast film production of PLLA/PDLA blend ratios

SC-PLA film has previously been made by solvent casting[19] into a masterbatch for injection molding[25,35] and for additive manufacturing.[24]

To the authors' knowledge, no published reports are available on producing SC-PLA film directly using cast film extrusion in a single screw extruder. This is likely due to a combination of differences in the flow characteristics of two enantiomeric resins and/or sub-optimal temperature profiles of the extruder. In this study, several blends of PLLA/PDLA resins with similar MFR, T_m, and similar M_n were combined and directly extruded in a single-screw extruder without the assistance of a master batch under the processing conditions indicated in Fig. S1.† The film combinations included 85/15, 70/30, 50/50, and 30/70 PLLA/PDLA and homopolymer PLLA and PDLA films for comparison purposes.

Fig. 1a shows images of the final films produced and the accompanying UV transmission values at 600 nm, indicating their transparency,[36] which were similar for all the films. Fig. S2 in the ESI† presents all the films' transmission rates *versus* wavelength.
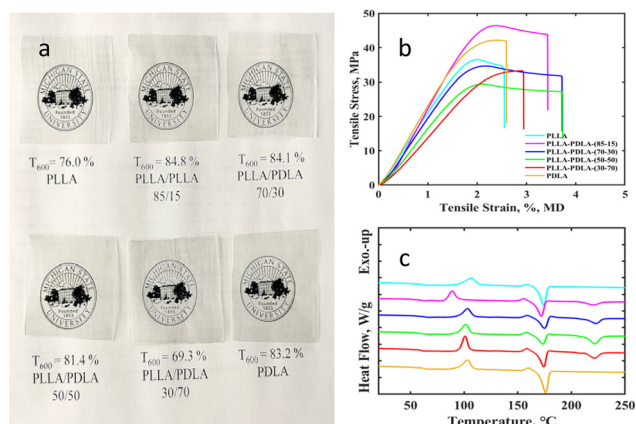
Fig. 1 (a) PLLA, PLLA/PDLA 85/15, 70/30, 50/50, 30/70, and PDLA films along with %T at 600 nm; (b) tensile strength of PLLA, blends, and PDLA in the machine direction (MD); (c) DSC of PLLA, blends, and PDLA. The identification legend in Fig. 1b carries over to Fig. 1c (*e.g.*, PLLA – light blue color in the online version of the manuscript).

Fig. 1b shows the stress *versus* strain characteristics of all the films in the MD. Fig. S3 in the ESI† shows the film's tensile strength in the CD. No significant differences were observed between the HC-PLA and the various blends. All the samples exhibited fragile behavior with low elongation at break. Table S4 in the ESI† presents the entire tensile characterization of the films. Improvement in tensile strength characteristics has been reported by others when SC-PLA samples were annealed or injection molded.[19,25] The extruded homopolymer films and the blends were extruded at about 230 °C. The resulting films were fully amorphous due to the low residence time. The process could not induce crystallinity as it cooled too quickly during the casting/chill process to allow crystallization to take place, as confirmed by DSC and WAXD (discussed in section 3.3). Fig. 1c shows the thermograms of PLLA, PDLA, and PLLA/PDLA blends as extruded, verifying minimal to no crystallization. As reported, the melting point of HC-PLA can be observed at around 175 °C and that of SC-PLA between 220 and 230 °C.[18] The PLLA and PDLA thermograms do not show melting peaks at about 220 °C since they are only HC-PLA. All the blends have the characteristic peak, with the 50/50 PLLA/PDLA blend having the most significant enthalpy depression due to the equimolar composition of L and D-PLA, maximizing the SC-PLA formation. The other four blends have an excess of either PLLA or PDLA and can only form the stereo-complex until one of them is fully consumed. Crystallization of SC-PLA in excess of PLLA or PDLA has been explored and reported. Brochu *et al.* studied a blend of 100L/80D, which allowed easier crystallization of the HC-PLA and, at the same time, potentially improved the formation of SC-PLA by isothermal crystallization.[37] Park and Hong reported that SC-PLA formation significantly promoted crystallinity and that the amount of PDLA dictated the crystallization of the PLLA/PDLA blend; as the amount of PDLA increased, the SC-X_c increased, with the equimolar blend having the highest amount of formed SC-PLA.[38] Schmidt and Hillmyer studied blends of PLLA with 0.25 to 15 weight percent optically pure PDLA and determined the blend ratio and the thermal treatment significantly modified the capability of the stereocomplex to nucleate the excess PLLA homopolymer. Also, the stereocomplex influenced the ensuing HC-PLLA crystallization. The amount of HC-PLA crystallization was lower than anticipated compared with the value of the pure homopolymer, attributed to the hindered mobility of the PLLA chains bound to the stereocomplex.[39]

3.2 Annealing the cast film

After the films were successfully produced, the effect of annealing was evaluated. The optimal annealing temperature was determined by running trials at 100, 140, 160, and 180 °C (data not shown). Annealing at temperatures higher than 160 °C made the film unusable since the HC-portion of the material melted. After reviewing the X_c data from the trials, it was established to use 160 °C as the annealing temperature. Fig. 2 shows the DSC thermograms and WAXD patterns of PLLA, blends of 70/30 and 50/50 PLLA/PDLA, and PDLA
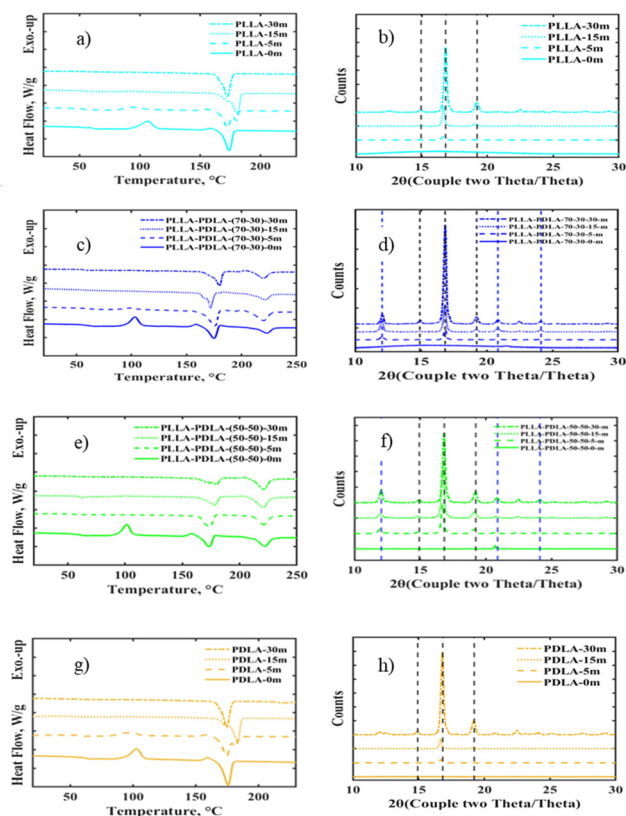
Fig. 2 (a) DSC thermograms of annealed PLLA-A-0,5,15,30 min; (b) WAXD patterns of annealed PLLA-A-0,5,15,30 min; (c) DSC thermograms of annealed PLLA-PDLA (70/30)-A-0,5,15,30 min; (d) WAXD patterns of annealed PLLA-PDLA (70/30)-A-0,5,15,30 min; (e) DSC thermograms of annealed PLLA-PDLA (50/50)-A-0,5,15,30 min; (f) WAXD patterns of annealed PLLA-PDLA (50/50)-A-0,5,15,30 min; (g) DSC thermograms of annealed PDLA-A-0,5,15,30 min; (h) WAXD patterns of annealed PDLA-A-0,5,15,30 min. *Note*: all DSC samples were annealed at 160 °C. In the WAXD patterns, the dashed black lines represent α-crystals, and the dashed blue lines represent SC-crystals.

obtained for 30, 15, 5, and 0 min at 160 °C. Fig. S4 in the ESI† shows the DSC thermograms and WAXD patterns obtained for the other blends, 85/15 and 30/70 PLLA/PDLA. Fig. 2b and h show that at 15 min, crystallization started in the PLLA and PDLA films, but full crystallization was not obtained until 30 minutes. All blends exhibited almost full crystallization at 5 min and complete saturation in crystal growth was observed at 15 min. The crystallization peaks at about 100 °C are absent at ≥5 min of annealing in Fig. 2c and e, indicating that complete crystallization is obtained for the blends with just 5 min of annealing or even less (data not shown). The WAXD patterns in Fig. 2d and f show distinct peaks corresponding to α-crystals (2Θ at 14.9°, 16.8°, and 19.2° associated with the 010, 110/220, and 203 crystal planes) and SC-crystals (2Θ at 12.0°, 20.8°, and 24.1° associated with the 110, 300/030 and 200 crystal planes) not present in the non-annealed samples.[40,41] Brochu et al.[37] reported the nucleating effect of PDLA on PLLA; they looked at PLLA/PDLA blends produced by solvent casting and showed that racemic crystallites formed

with as little as 10% PDLA. This finding is consistent with the findings of Tsuji and Ikada,[19] indicating that a 50/50 PLLA/PDLA blend produced *via* solvent casting had complete crystallization at 5 min, while PLLA and PDLA did not show appreciable crystallization until 10 min. Our work shows that complete crystallization can be achieved in cast films with a 50/50 PLLA/PDLA blend and the other blends (85/15, 70/30, and 30/70 PLLA/PDLA) at even 5 min, and maybe even less.

Fig. 3 shows the tensile stress *versus* strain for the 70/30 and 85/15 PLLA/PDLA blends after annealing at different times. The film strength dropped dramatically in the MD and CD at 5 and 15 min due to increased brittleness. The tensile stress and strain of the two blends were no better than those of the HC-PLA samples after extruding (data not shown). Table S4 in the ESI† summarizes non-annealed tensile stress and strain for all the films. By annealing the samples, the crystallinity was increased to 16–47%, depending on the annealing time, analyzed *via* WAXD. Park and Hong also reported tensile curves of PLLA/PDLA blended films, indicating a brittle material with no yield point or plastic deformation;[38] samples annealed at 30 min could not be measured due to their brittleness. Table 1 summarizes the tensile stress and strain results for the two blends and shows that all the annealed samples had significantly lower tensile stress and tensile strain than the non-annealed samples; most annealed samples were not significantly different ($P > 0.05$). Suder et al. reported that the tensile strength of PLA increased with increasing annealing temperature, with a maximum increase at 100 °C; however, as the annealing temperature went above 100 °C, the tensile strength decreased and was even lower compared with the
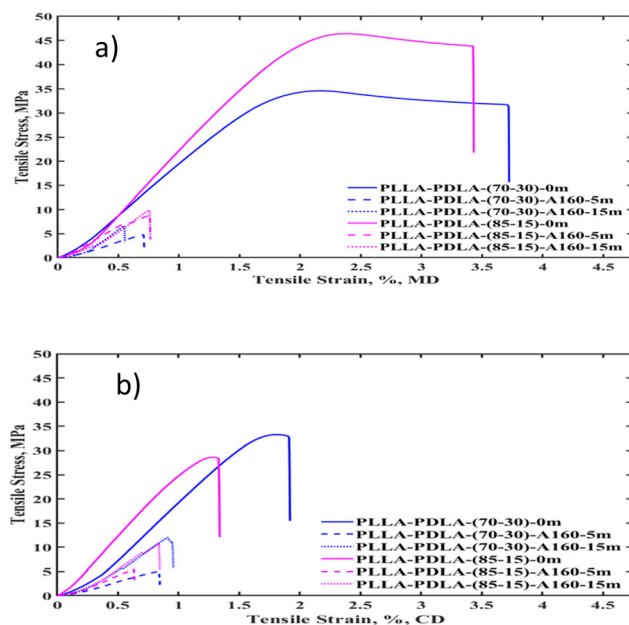
Fig. 3 Stress *versus* strain at 160 °C and various annealing times for (a) PLLA/PDLA (70/30) and PLLA/PDLA (85/15)– machine direction(MD), and (b) PLLA/PDLA (70/30) and PLLA/PDLA (85/15) – cross direction (CD).

Table 1 Summary of tensile stress and stain for PLLA/PDLA (70/30) and PLLA/PDLA (85/15) at varying annealing times

	Tensile stress at Maximum load		Tensile strain at tensile strength	
	MD	CD	MD	CD
Material	MPa	MPa	%	%
PLLA/PDLA(70/30)–0 minutes	35.49 ± 2.66[a]	30.19 ± 3.93[d]	2.34 ± 0.14[f]	1.82 ± 0.16[h]
PLLA/PDLA(70/30) A160–5 minutes	5.15 ± 1.25[b]	5.49 ± 2.23[e]	0.74 ± 0.14[g]	0.86 ± 0.14[i]
PLLA/PDLA(70/30) A160–15 minutes	5.37 ± 1.36[b]	8.21 ± 2.38[e]	0.6 ± 0.06[g]	0.93 ± 0.10[i]
PLLA/PDLA(85/15)–0 minutes	43.97 ± 4.94[c]	28.77 ± 1.15[d]	2.42 ± 0.22[f]	1.33 ± 0.10[j]
PLLA/PDLA(85/15) A160–5 minutes	8.80 ± 3.54[b]	5.63 ± 1.82[e]	0.73 ± 0.10[g]	0.63 ± 0.11[k]
PLLA/PDLA(85/15) A160–15 minutes	5.70 ± 2.91[b]	8.10 ± 1.22[e]	0.73 ± 0.19[g]	0.86 ± 0.22[i]

Values are means ± SD (n = 8); within columns, means with different letters are significantly different at $P \leq 0.05$ (Tukey–Kramer test). Values at 30 min could not be obtained.

non-annealed samples.[42] The samples in this study were all annealed at 160 °C to maximize crystallization and nucleation of SC. The data collected from the trials mentioned above supported the annealing temperature chosen. The process of annealing the samples had a beneficial effect on inducing crystallinity but had a detrimental impact on the film's overall strength. However, samples with 5 min of annealing time provide sufficient crystallization to tailor other properties, such as moisture vapor transmission rate, discussed in the next section.

3.3 Moisture vapor barrier characteristics

Annealed and non-annealed samples were evaluated for moisture vapor transmission to confirm the benefit of the increased crystallinity. The moisture vapor permeability coefficient (MVPC) for PLLA, PDLA, and all the blends annealed at 30 min was compared. Fig. 4 summarizes the results and shows that all the annealed samples had significantly better (lower) MVPCs than the non-annealed samples; however, there was no difference among any of the annealed samples. Increasing the crystallinity generally reduces a polymer's solubility, diffusion, and permeability.[43] In this case, the increase of crystallinity directly affected the reduction in MVPC. In addition, the inter-

mediate blends of PLLA/PDLA (85/15, 70/30, 50/50, and 30/70) also resulted in significantly improved barriers. Shogren reported the MVTR of a solvent-casted PLLA film to be more than double that of an annealed film at 54 °C for 10 min,[44] consistent with the results in Fig. 4. Siparsky et al. reported on the barrier of solvent-casted PLLA and PLLA/PDLA blends ranging in X_c from 0 to 46%; the permeability coefficients of the three annealed samples measured at 38 °C/90% RH were lower than the non-annealed ones,[45] indicating a similar trend as we observed in this study.

The effect of annealing time was explored as it relates to the MVPC and X_c. Fig. 5 shows the MVPC for each treatment and indicates whether the sample is amorphous (A) and the HC-PLA and SC-PLA crystalline ratio, where applicable.

Table 2 summarizes the MVPC for each treatment and includes the X_c obtained by DSC and WAXD for each annealing time. There was a direct correlation between the improved barrier and the overall percentage of crystallinity. The same trend discussed earlier concerning crystallinity at the various annealing times also appears valid for the MVPC. The blended non-annealed samples significantly differ from the annealed
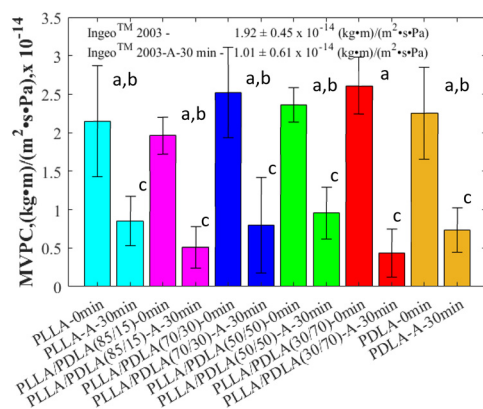
Fig. 4 Moisture vapor permeability coefficients for all blends evaluated annealed at 0 and 30 minutes. *Note*: values followed by a different letter are significantly different at $P \leq 0.05$ (Tukey–Kramer test).
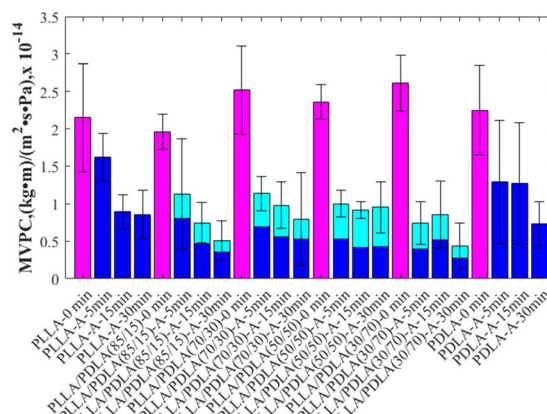
Fig. 5 Moisture vapor permeability coefficients for all blends evaluated annealed at 0,5, 15, and 30 min. The magenta bars represent amorphous samples, the blue bars represent the HC-PLA crystalline portion, and the cyan bars represent the SC-PLA crystalline portion.

Table 2 Moisture vapor permeability coefficients for PDLA, PLLA, various blends, and DSC and WAXD crystallinity values

Material	MVPC		DSC				WAXD			
	n	$((kg\ m)/(m^2\ s\ Pa)) \times 10^{-14}$	$X_{c,HC}$	$X_{c,SC}$	$X_{c,t}$	% SC	$Xc\text{-}\alpha$	$X_{c,SC}$	$X_{c,t}$	% SC
PLLA-A160-30 min	12	$0.853 \pm 0.324^{e,f}$	41	—	41	—	31	—	31	—
PLLA-A160-15 min	12	$0.892 \pm 0.233^{e,f}$	42	—	42	—	26	—	26	—
PLLA-A160-5 min	9	$1.62 \pm 0.320^{a,c,d}$	27	—	27	—	16	—	16	—
PLLA-A160-0 min	14	$2.15 \pm 0.720^{a,b}$	0	—	0	—	0	—	0	—
PLLA/PDLA(85/15)-A160-30 min	10	0.508 ± 0.269^{f}	31	14	44	31	34	8	42	19
PLLA/PDLA(85/15)-A160-15 min	12	$0.744 \pm 0.3260^{e,f}$	26	15	41	38	29	13	42	30
PLLA/PDLA(85/15)-A160-5 min	14	$1.130 \pm 0.590^{d,e,f}$	29	12	41	28	23	5	28	18
PLLA/PDLA(85/15)-A160-0 min	8	$1.960 \pm 0.240^{a,b,c,d}$	0	0	0	—	0	0	0	—
PLLA/PDLA(70/30)-A160-30 min	23	$0.798 \pm 0.617^{e,f}$	28	15	42	35	24	12	36	34
PLLA/PDLA(70/30)-A160-15 min	7	$0.981 \pm 0.312^{e,f}$	22	17	39	44	20	13	33	40
PLLA/PDLA(70/30)-A160-5 min	10	$1.140 \pm 0.230^{d,e,f}$	30	19	49	39	29	5	34	14
PLLA/PDLA(70/30)-A160-0 min	8	2.520 ± 0.590^{b}	0	0	0	—	0	0	0	—
PLLA/PDLA(50/50)-A160-30 min	21	$0.953 \pm 0.341^{e,f}$	19	24	42	56	15	22	37	59
PLLA/PDLA(50/50)-A160-15 min	8	$0.918 \pm 0.113^{e,f}$	21	25	47	54	40	7	47	15
PLLA/PDLA(50/50)-A160-5 min	10	$0.998 \pm 0.179^{e,f}$	26	22	48	47	38	7	45	16
PLLA/PDLA(50/50)-A160-0 min	9	$2.36 \pm 0.230^{a,b}$	0	0	0	—	0	0	0	—
PLLA/PDLA(30/70)-A160-30 min	8	0.433 ± 0.310^{f}	29	17	46	37	25	7	32	21
PLLA/PDLA(30/70)-A160-15 min	8	$0.856 \pm 0.450^{e,f}$	26	17	43	40	22	13	35	37
PLLA/PDLA(30/70)-A160-5 min	10	$0.741 \pm 0.287^{e,f}$	18	16	34	47	11	12	23	51
PLLA/PDLA(30/70)-A160-0 min	15	2.61 ± 0.370^{b}	0	0	0	—	0	0	0	—
PDLA-A160-30 min	8	$0.732 \pm 0.293^{e,f}$	43	—	43	—	37	—	37	—
PDLA-A160-15 min	6	$1.270 \pm 1.530d^{,e,f}$	48	—	48	—	21	—	21	—
PDLA-A160-5 min	6	$1.290 \pm 0.820^{c,d,e,f}$	34	—	34	—	22	—	22	—
PDLA-A160-0 min	7	$2.250 \pm 0.600^{a,b,c}$	0	—	0	—	0	—	0	—

MVPC values are means ± SD; means followed by a different letter are significantly different at $P \leq 0.05$ (Tukey–Kramer test). DSC and WAXD measured crystallinity. WAXD is the ratio of the crystalline peaks' area to the diffraction pattern's total size. The crystalline peak areas were obtained by subtracting the amorphous halo from the entire peak areas.

blend composition for all annealing times *i.e.* 5, 15, and 30 min. The PLLA samples do not vary considerably from the non-annealed sample until 15 min of annealing time. The 15 min and 30 min annealed PDLA samples show a significant difference from the non-annealed sample; however, the 5 min PDLA sample does not differ significantly from the other PDLA samples. Tsuji *et al.* reported that the MVPC of PLLA films decreased monotonically as the X_c increased from 0 to 20% but leveled off at X_c greater than 30%. The finding was attributed to the elevated production of RAF regions to moisture permeation compared with the MAF regions.[46] All our annealed samples had an X_c greater than 30%, with no significant difference. Tsuji and Tsuruno reported the MVPC for PLLA, PDLA, and a blend of (50/50) PDLA/PLLA for solvent-cast film and observed a similar trend where all three films markedly improved with annealing; the values reported ranged from 1.00 to 2.29 $((kg\ m)/(m^2\ s\ Pa)) \times 10^{-14}$,[23] like our reported values. Our work further demonstrated that the intermediate blends of PLLA/PDLA (85/15, 70/30, and 30/70) also resulted in significantly improved barriers. This finding means that improvement is obtained with as low as 15% PDLA, which should be commercially beneficial since PLLA is more economical and commercially available than PDLA at present.

The WAXD crystallinity was decoupled between the α-crystal and the SC-crystal by looking at the various peaks. The peaks at 2θ = 14.9, 16.8, and 19.2 correspond to the α-crystal. The peaks at 2θ = 12.0, 20.8, and 24.1 correspond to the SC-crystal.[41,47] As shown in Fig. 5, the α-crystal dominates in all the blends except the 50/50 PLLA/PDLA blend. In the PLLA/PDLA 50/50 scenario, equal amounts of PLLA and PDLA can maximize the interactivity between the two enantiomeric materials, increasing the amount of SC-PLA formed. Hence, the 50/50 blend has the highest SC-PLA amount of all the samples. In all other combinations, PLLA or PDLA is present at different levels, limiting the reaction between the two and leaving an abundance of unreacted PLLA or PDLA, depending on the blend ratio. This does not stop the remaining PLLA or PDLA from forming α-crystal at the annealing temperature/time combination. The overall WAXD $X_{c,t}$ for all the annealed materials ranges from 16% to 47%, depending on the annealing time. The MVPC is also about the same for all the annealed samples since there is no significant difference between the annealed blended samples or the HC-PLA annealed samples at 15 min of annealing or more. Chen *et al.* reported similar findings on SC-PLA and the distribution between the formation of α-crystals and SC-crystals; they reported that at 140 °C, the α-crystals formed in a much higher abundance than SC-crystals.[41] This study was conducted at 160 °C but yielded similar findings, which means the overall X_C improves the barrier more than the individual X_{HC} or X_{SC} formed. Additional studies could be conducted to decouple the role of the α-crystals and the SC-crystals. Maybe selective film manipulation could further improve the properties of final films.

4. Conclusion

SC-PLA was produced using cast film extrusion directly in a single-screw extruder without first producing a masterbatch. This is an excellent first step in producing commercial SC-PLA film in one process. We annealed the SC-PLA film with a hydraulic press at a lab-scale level, but the same results could be obtained by orienting in line on a commercial scale while casting the film due to the fast conversion times. The barrier properties were improved from 2.5 to 6 times with annealing, depending on the film, including PLLA and PDLA, indicating that annealing alone can improve MVPC. This is a superior MVPC compared to other compostable options and is a good first step for a high moisture barrier film compared to its petrochemical-based counterparts. However, stereocomplexation decreases the annealing time needed to induce crystallization and subsequent MVPC improvement. Improvement of MVPC characteristics can be achieved with as little as 15% PDLA, which is highly beneficial since PLLA is the more commercially available of the two stereoisomers, helping with the economics due to the price and availability of PDLA compared to PLLA in the marketplace. The total formed crystallinity dictates the improved MVPC and not the contribution of either the homo or stereocomplex crystals. Even though the increased crystallinity improved the MVPC, it had a detrimental effect on the strength characteristics. Future work should be conducted to tailor the brittleness while maintaining the improved MVPC values.

Author contributions

James F. Macnamara Jr.: conceptualization, investigation, formal analysis, visualization, writing – original draft, review & editing. Maria Rubino: conceptualization, writing – review & editing. Matthew Daum: conceptualization, writing – review & editing. Ajay Kathuria: conceptualization, writing – review & editing. Rafael Auras: conceptualization, writing – original draft, review & editing, supervision, funding acquisition. All the authors approved the final version for submission.

Conflicts of interest

The authors declare that they have no known competing financial interests or personal relationships that could have appeared to influence the work reported in this paper.

Acknowledgements

References

1 Global Packaging Film Market Report 2020: Analysis & Forecasts 2012–2019 & 2020–2027 by LDPE, HDPE, BOPP, Polyester, PVC, Polyamide, EVOH - ResearchAndMarkets.com [Internet]. [cited 2022 Aug 1]. Available from: **https://www.businesswire.com/news/home/20210211005672/en/Global-Packaging-Film-Market-Report-2020-Analysis-Forecasts-2012-2019-2020-2027-by-LDPE-HDPE-BOPP-Polyester-PVC-Polyamide-EVOH–ResearchAndMarkets.com**.

2 Flexible Packaging Market Size Worth $373.3 Billion By 2030 [Internet]. [cited 2022 Aug 20]. Available from: **https://www.businesswire.com/news/home/20231026140229/en/Global-Flexible-Packaging-Market-Set-to-Reach-USD-373.34-Billion-by-2030-Marking-Steady-Growth-at-4.7-CAGR–ResearchAndMarkets.com#:~:text=The%20global%20flexible%20packaging%20market,4.7%25%20from%202023%20to%202030**.

3 Plastics_ Material-Specific Data _ US EPA [Internet]. 2022 [cited 2022 Oct 18]. Available from: **https://www.epa.gov/facts-and-figures-about-materials-waste-and-recycling/plastics-material-specific-data**.

4 Design for sustainability_ understanding compostable plastic packaging [Internet]. [cited 2022 Aug 17]. Available from: **https://nutraceuticalbusinessreview.com/news/article_page/Design_for_sustainability_understanding_compostable_plastic_packaging/202066**.

5 M. Murariu and P. Dubois, *PLA composites: From production to properties. Vol. 107, Advanced Drug Delivery Reviews*, Elsevier B.V., 2016, pp. 17–46.

6 One word, bioplastics: Investments pour into biodegradable plastic [Internet]. 2022 [cited 2023 Jun 19]. Available from: **https://www.csmonitor.com/Environment/2022/0810/One-word-bioplastics-Investments-pour-into-biodegradable-plastic**.

7 Y. Li, Z. Qiang, X. Chen and J. Ren, Understanding thermal decomposition kinetics of flame-retardant thermoset polylactic acid, *RSC Adv.*, 2019, **9**(6), 3128–3139.

8 H. Bai, C. Huang, H. Xiu, Q. Zhang, H. Deng, K. Wang, *et al.*, Significantly Improving Oxygen Barrier Properties of Polylactide via Constructing Parallel-Aligned Shish-Kebab-Like Crystals with Well-Interlocked Boundaries, *Biomacromolecules*, 2014, **15**(4), 1507–1514.

9 I. S. M. A. Tawakkal, M. J. Cran, J. Miltz and S. W. Bigger, A Review of Poly(Lactic Acid)-Based Materials for Antimicrobial Packaging, *J. Food Sci.*, 2014, **79**(8), 1477–1490.

10 L. Deng, C. Xu, X. Wang and Z. Wang, Supertoughened Polylactide Binary Blend with High Heat Deflection Temperature Achieved by Thermal Annealing above the Glass Transition Temperature, *ACS Sustainable Chem. Eng.*, 2018, **6**(1), 480–490.

11 M. Wang, Y. Wu, Y. D. Li and J. B. Zeng, *Progress in Toughening Poly(Lactic Acid) with Renewable Polymers. Vol. 57*, Polymer Reviews, Taylor and Francis Inc., 2017, pp. 557–593.

12 V. Speranza, A. De Meo and R. Pantani, Thermal and hydrolytic degradation kinetics of PLA in the molten state, *Polym. Degrad. Stab.*, 2014, **100**(1), 37–41.

13 RM Rasal, A v. Janorkar and DE Hirt, *Poly(lactic acid) modifications. Vol. 35, Progress in Polymer Science*, Oxford, 2010, pp. 338–356.

14 S Singha and MS Hedenqvist, *A review on barrier properties of poly(lactic Acid)/clay nanocomposites. Vol. 12, Polymers. MDPI AG*, 2020.

15 Y. Ikada, K. Jamshidi, H. Tsuji and S. H. Hyon, Stereocomplex Formation between Enantiomeric Poly(lactides), *Macromolecules*, 1987, **20**(4), 904–906.

16 T. Okihara, M. Tsuji, A. Kawaguchi, K. I. Katayama, H. Tsuji, S. H. Hyon, *et al.*, Crystal structure of stereocomplex of poly(L-lactide) and poly(D-lactide), *J. Macromol. Sci., Part B: Phys.*, 1991, **30**, 119–140. Available from: https://www.tandfonline.com/action/journalInformation?journalCode=lmsb20.

17 Z. Q. Wan, J. M. Longo, L. X. Liang, H. Y. Chen, G. J. Hou, S. Yang, *et al.*, Comprehensive Understanding of Polyester Stereocomplexation, *J. Am. Chem. Soc.*, 2019, **141**(37), 14780–14787.

18 H. Tsuji, *Poly(lactide) stereocomplexes: Formation, structure, properties, degradation, and applications. Vol. 5, Macromolecular Bioscience*, Wiley-VCH Verlag, 2005, pp. 569–597.

19 H. Tsuji and Y. Ikada, Stereocomplex formation between enantiomeric poly(lactic acid)s. XI. Mechanical properties and morphology of solution-cast films, *Polymer*, 1999, **40**, 6699–6708.

20 H. Shirahama, A. Ichimaru, C. Tsutsumi, Y. Nakayama and H. Yasuda, Characteristics of the Biodegradability and Physical Properties of Stereocomplexes between Poly(L-lactide) and Poly(d-lactide) Copolymers, *J. Polym. Sci., Part A: Polym. Chem.*, 2005, **43**(2), 438–454.

21 Materials Part 1_ What Annealing Can Do for Your Process _ Plastics Technology [Internet]. [cited 2022 Aug 25]. Available from: https://www.ptonline.com/blog/post/materials-part-1-what-annealing-can-do-for-your-process.

22 A. Guinault, C. Sollogoub, S. Domenek, A. Grandmontagne and V. Ducruet, Influence of Crystallinity on Gas Barrier and Mechanical Properties of PLA Food Packaging Films, *Int. J. Mater. Form.*, 2010, **3**(Suppl. 1), 603–606.

23 H. Tsuji and T. Tsuruno, Water Vapor Permeability of Poly(L-lactide)/Poly(D-lactide) Stereocomplexes, *Macromol. Mater. Eng.*, 2010, **295**(8), 709–715.

24 F. Luo, A. Fortenberry, J. Ren and Z. Qiang, *Recent Progress in Enhancing Poly(Lactic Acid) Stereocomplex Formation for Material Property Improvement. Vol. 8, Frontiers in Chemistry*, Frontiers Media S.A., 2020.

25 M. Alhaj and R. Narayan, Scalable Continuous Manufacturing Process of Stereocomplex PLA by Twin-Screw Extrusion, *Polymers*, 2023, **15**(4), 922.

26 PDLA Polymer Supplier and Manufacturer in China [Internet]. [cited 2022 May 12]. Available from: https://polylactide.com/polyd-lactide/.

27 H. S. Lee, E. H. Kim and J. D. Kim, Effect of Stereocomplex Crystallite as a Nucleating Agent on the Isothermal Crystallization Behavior of Poly(L-Lactic Acid), *Plast. Eng.*, 2013, **2**(9), 937–943.

28 PRODUCT DATA SHEET LUMINY ® L130 Product Data Sheet Luminy® L130 [Internet]. 2019. Available from: https://www.totalenergies-corbion.com.

29 PRODUCT DATA SHEET LUMINY ® D120 Product Data Sheet Luminy® D120 [Internet]. 2022. Available from: https://www.totalenergies-corbion.com.

30 Product Data Sheet Luminy® L175 [Internet]. 2019 May. Available from: https://www.total-corbion.com.

31 PRODUCT DATA SHEET LUMINY ® D070 Product Data Sheet Luminy® D070 [Internet]. 2019 May. Available from: https://www.total-corbion.com.

32 ASTM D1238–20 Standard Test Method for Melt Flow Rates of Thermoplastics by Extrusion Plastometer 1 [Internet]. West Conshohocken, 2020. Available from: https://www.ansi.org.

33 ASTM F1249–20 Standard Test Method for Water Vapor Transmission Rate Through Plastic Film and Sheeting Using a Modulated Infrared Sensor [Internet]. West Conshohocken, 2020. Available from: https://www.astm.org.

34 Standard Test Method for Tensile Properties of Thin Plastic Sheeting 1. Available from: https://www.ansi.org.

35 H. Bai, S. Deng, D. Bai, Q. Zhang, Q. Fu and H. W. Bai, *et al.*, *REVIEW 1700454 (1 of 12) Recent Advances in Processing of Stereocomplex-Type Polylactide*, 2017. Available from: https://www.advancedsciencenews.com.

36 Standard Test Method for Transparency of Plastic Sheeting [Internet]. 2023. Available from: https://www.astm.org.

37 S. Brochu, R. E. Prud'homme, I. Barakat and R. Jerome, Stereocomplexation and Morphology of Polylactides, *Macromolecules*, 1995, **28**(15), 5230–5239.

38 H. S. Park and C. K. Hong, Relationship between the Stereocomplex Crystallization Behavior and Mechanical Properties of PLLA/PDLA Blends, *Polymers*, 2021, **13**(11), 1851.

39 S. C. Schmidt and M. A. Hillmyer, Polylactide Stereocomplex Crystallites as Nucleating Agents for Isotactic Polylactide, *J. Polym. Sci., Part B: Polym. Phys.*, 2001, **39**, 300–313.

40 P. Pan, L. Han, J. Bao, Q. Xie, G. Shan and Y. Bao, Competitive Stereocomplexation, Homocrystallization, and Polymorphic Crystalline Transition in Poly(L-lactic acid)/Poly(D-lactic acid) Racemic blends: Molecular Weight Effects, *J. Phys. Chem. B*, 2015, **119**(21), 6462–6470.

41 Q. Chen, R. Auras, J. K. Kirkensgaard and I. Uysal-Unalan, Modulating Barrier Properties of stereocomplex Polylactide: The Polymorphism Mechanism and its Relationship with Rigid Amorphous Fraction, *ACS Appl. Mater. Interfaces*, 2023, **15**, 49678–49688.

42 J. Suder, Z. Bobovsky, Z. Zeman, J. Mlotek and M. Vocetka, The Influence of Annealing Temperature on Tensile Strength of Polylactic Acid, *MM Sci. J.*, 2020, 4132–4137.

43 C.E. Rogers, in *Polymer Permeability*, J. Comyn, Chapman and Hall, London, 1985. Available from: https://link.springer.com/10.1007/978-94-009-4858-7.

44 R. Shogren, Water Vapor Permeability of Biodegradable Polymers, *J. Environ. Polym. Degrad.*, 1997, **5**(2), 91–95.

45 G. L. Siparsky, K. J. Voorhees, J. R. Dorgan and K. Schilling, Water Transport in Polylactic Acid (PLA), PLA/Polycaprolactone Copolymers, and PLA/Polyethylene Glycol Blends, *J. Environ. Polym. Degrad.*, 1997, **5**(3), 125–136.

46 H. Tsuji, R. Okino, H. Daimon and K. Fujie, Water Vapor Permeability of Poly(lactide)s: Effects of Molecular Characteristics and Crystallinity, *J. Appl. Polym. Sci.*, 2006, **99**(5), 2245–2252.

47 B. Ma, H. Zhang, K. Wang, H. Xu, Y. He and X. Wang, Influence of scPLA microsphere on the crystallization behavior of PLLA/PDLA composites, *CompComm*, 2020, **21**, 100380.